

## Loss-of-Function Mutations in *Euchromatin Histone Methyl Transferase 1 (EHMT1)* Cause the 9q34 Subtelomeric Deletion Syndrome

Tjitske Kleefstra, Han G. Brunner, Jeanne Amiel, Astrid R. Oudakker, Willy M. Nillesen, Alex Magee, David Geneviève, Valérie Cormier-Daire, Hilde van Esch, Jean-Pierre Fryns, Ben C. J. Hamel, Erik A. Sistermans, Bert B. A. de Vries, and Hans van Bokhoven

A clinically recognizable 9q subtelomeric deletion syndrome has recently been established. Common features seen in these patients are severe mental retardation, hypotonia, brachycephaly, flat face with hypertelorism, synophrys, anteverted nares, cupid bow or tented upper lip, everted lower lip, prognathism, macroglossia, conotruncal heart defects, and behavioral problems. The minimal critical region responsible for this 9q subtelomeric deletion (9q<sup>-</sup>) syndrome has been estimated to be <1 Mb and comprises the *euchromatin histone methyl transferase 1* gene (*EHMT1*). Previous studies suggested that haploinsufficiency for *EHMT1* is causative for 9q subtelomeric deletion syndrome. We have performed a comprehensive mutation analysis of the *EHMT1* gene in 23 patients with clinical presentations reminiscent of 9q subtelomeric deletion syndrome. This analysis revealed three additional microdeletions that comprise the *EHMT1* gene, including one interstitial deletion that reduces the critical region for this syndrome. Most importantly, we identified two de novo mutations—a nonsense mutation and a frameshift mutation—in the *EHMT1* gene in patients with a typical 9q<sup>-</sup> phenotype. These results establish that haploinsufficiency of *EHMT1* is causative for 9q subtelomeric deletion syndrome.

Submicroscopic subtelomeric deletions of chromosome 9q have been reported in 30 individuals, and this number has been rapidly increasing since it was found recently that such deletions are associated with a recognizable mental retardation (MR) syndrome.<sup>1–8</sup> Common features in patients with 9q subtelomeric deletion syndrome are severe MR, hypotonia, brachy(micro)cephaly, epileptic seizures, flat face with hypertelorism, synophrys, anteverted nares, everted lower lip, carp mouth with macroglossia, and heart defects. The minimal critical region responsible for this 9q subtelomeric deletion phenotype (9q<sup>-</sup>) was originally estimated to be ~1 Mb.<sup>1,4</sup> This region was subsequently reduced to an ~700-kb region that contains at least five genes—*ZMYND19*, *ARRDC1*, *C9ORF37*, *EHMT1*, and *CACNA1B*—and several spliced ESTs<sup>8</sup> (fig. 1). In the latter study,<sup>8</sup> a genotype-phenotype analysis was performed with 15 individuals and their associated sizes of 9q34.3 deletions. This study suggested that haploinsufficiency for one or more genes in the ~700-kb critical region is responsible for the common clinical findings of 9q34.3 subtelomeric deletion syndrome—craniofacial dysmorphic features, hypotonia, obesity, microcephaly, and speech anomalies, which were designated by the authors as “CHOMS.” Other manifestations, such as cardiac defects, seizures, limb and brain anomalies, recurrent respiratory infections, hypothyroidism, and abnormal genitalia, were more common in individuals with larger de-

letions, which led to the hypothesis that these characteristics were due to the deletion of one or more proximally located genes. However, in a recent study, we postulated that haploinsufficiency of the *EHMT1* gene, which encodes euchromatin histone methyltransferase 1 (EhMTase1 [MIM 607001]), was responsible for 9q<sup>-</sup> syndrome.<sup>6</sup> Characterization of the breakpoints in a female with a balanced translocation t(X;9)(p11.23;q34.3) revealed that the chromosome 9 breakpoint disrupted the *EHMT1* gene in intron 9. The patient presented typical features of 9q subtelomeric deletion syndrome, including severe MR, facial dysmorphisms, cardiac anomaly, seizures, hearing loss, and behavioral problems. Thus, this result suggested that subtelomeric 9q34.3 deletion syndrome is not a contiguous gene syndrome but that the core phenotype of this recognizable entity is due to haploinsufficiency of just one gene: *EHMT1*.

To find additional evidence for the causative role of the *EHMT1* gene, we performed mutation analysis in patients with a clinical presentation reminiscent of 9q subtelomeric deletion syndrome. This analysis provides compelling evidence for the causative role of the *EHMT1* gene in 9q subtelomeric deletion syndrome.

Our study was performed on DNA from 23 patients with MR with additional features seen in 9q<sup>-</sup> syndrome. Minimal inclusion criteria were severe MR and suggestive craniofacial dysmorphic features. However, most patients also

From the Department of Human Genetics, Radboud University Nijmegen Medical Centre, Nijmegen, The Netherlands (T.K.; H.G.B.; A.R.O.; W.M.N.; B.C.J.H.; E.A.S.; B.B.A.d.V.; H.v.B.); Department of Human Genetics, Hôpital Necker Enfants-Malades, Paris (J.A.; D.G.; V.C.-D.); Regional Genetics Service, Belfast City Hospital Trust, Belfast (A.M.); and Center for Human Genetics, University Hospital, Leuven, Belgium (H.v.E.; J.-P.F.)

Received April 7, 2006; accepted for publication May 8, 2006; electronically published June 13, 2006.

Address for correspondence and reprints: Dr. T. Kleefstra, Department of Human Genetics 849, Radboud University Nijmegen Medical Centre, P.O. Box 9101, 6500 HB Nijmegen, The Netherlands. E-mail: T.Kleefstra@antrg.umcn.nl

*Am. J. Hum. Genet.* 2006;79:370–377. © 2006 by The American Society of Human Genetics. All rights reserved. 0002-9297/2006/7902-0020\$15.00

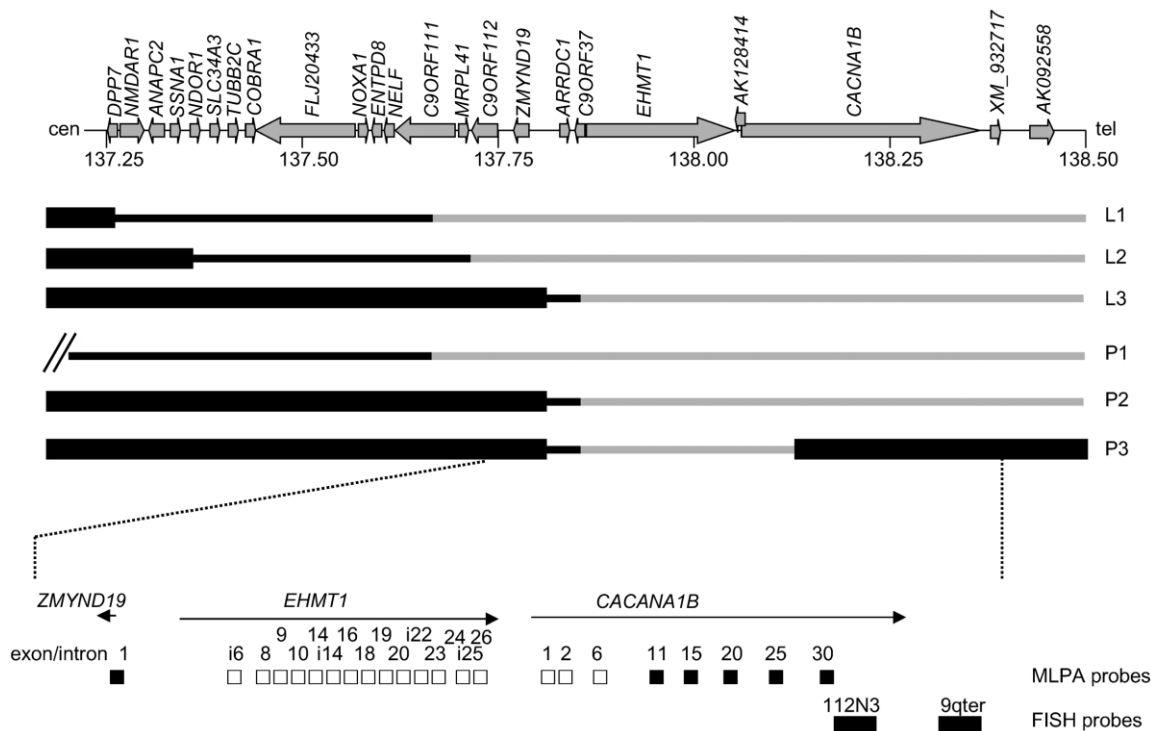


**Figure 1.** Deletions of chromosome 9q34.3 identified in individuals with 9q subtelomeric deletion syndrome. The top bar is the genomic organization of the relevant region in 9q34.3. The sizes and orientations of the known and predicted genes are indicated by gray arrows. The sizes of the deletions reported elsewhere (L1–L3) and the new deletions identified in this study (P1–P3) are represented by the bars. Gray lines are deleted regions, and the thick bars represent the regions with normal copy numbers. The intervening regions are indicated by black lines. Deletions reported elsewhere are redrawn from Stewart et al.<sup>4</sup> (L1), Harada et al.<sup>2</sup> (L2), and Yatsenko et al.<sup>8</sup> (L3). A large deletion of at least 1 Mb, with the proximal border between the *tMRPL41* gene and the *TRAF2* gene, was identified in patient P1. The deletion in P2 is similar to the critical region indicated by L3. P3 has a smaller interstitial deletion. The size of the deletion was determined by FISH analysis and MLPA (lower panel). Unblackened boxes indicate probes located in exons or introns (i) with reduced (~50%) signal intensity, whereas the blackened boxes represent probes with normal intensities.

presented other features of 9q<sup>-</sup> syndrome. All were previously screened for submicroscopic telomeric deletions, by either FISH with routine telomeric probes or by multiplex ligation-dependent probe amplification (MLPA) with routine probes.<sup>9</sup> After we obtained informed consent, genomic DNA was extracted from peripheral blood lymphocytes by a salt-extraction procedure.<sup>10</sup>

Initial MLPA analysis was performed using the standard kits SALSA P019 or P036 Human Telomere Test Kit (MRC-Holland), as described by Schouten et al.,<sup>11</sup> with slight modifications. Subsequent MLPA analyses were performed with the recently developed P070 MRC-Holland kit containing a probe matching exon 9 of the *EHMT1* gene. These MLPAs provided evidence for 9q subtelomeric deletions in three of the patients. These three patients had a signal intensity of ~50%. Patient 1 also had a decreased signal for the *MRPL41* probe and a normal signal at *TRAF2*, which is indicative of a deletion exceeding the size of the critical region defined elsewhere.<sup>8</sup> However, patients 2 and 3 had a normal signal intensity for the *MRPL41* probe, suggesting the presence of a smaller deletion. To verify these results and to fine-map the size of the deletions, we

developed additional MLPA probes within the critical interval for 9q<sup>-</sup> syndrome (fig. 1). Probe preparation has been described elsewhere.<sup>9</sup> The newly designed MLPA probes covered exon 1 of *ZMYND19*, which is the most distally located exon, and several exons or introns of both *EHMT1* and *CACNA1B* (table 1). Unfortunately, no suitable probes for *ARRDC1* and *C9ORF37* could be developed. Results obtained with these additional MLPA probes confirmed the presence of a heterozygous deletion in all three patients. Patients 2 and 3 had a decreased signal for all probes in the *EHMT1* gene. The proximal-flanking probe in exon 1 of *ZMYND19* was not deleted in either of these two patients, which indicated that the maximum size of the deletion is 670 kb. The deletion in patient 2 has a size similar to the critical region defined by Yatsenko et al.<sup>8</sup> and comprises *ARRDC1*, *C9ORF37*, *EHMT1*, *CACNA1B*, and the ESTs represented by AK128414 and AK092558 and by XM\_932717, which encodes a protein that is highly similar to isoform 2 of  $\beta$ -tubulin 8 (UNILIB and UCSC Genome Browser). The deletion in patient 3 is even smaller, since only exons 1–6 of *CACNA1B* were deleted. Probes in exons 11, 15, 20, 25, and 30 of *CACNA1B*

**Table 1. Sequences of MLPA Probes**

Gene <sup>a</sup>	Primer (5'→3')	
	Forward	Reverse
ZMYND19_e1	GCCGTCGTTTACACCCGGCCATGACCGACTTCAA	ATTGGGTATCGTGC GGCTCGGCAGGAAACAGCTAT
EHMT1_i6	CACCAGCGTCTTCAGTTCTT	TACCCAACAACCTTGTGTC
EHMT1_e8	CCAGGAGACAGCACAGGGTACAT	GGAAAGTTTCTCTGGACTCCCTGG
EHMT1_e9	CCAGATGTGCTGGAGACAGACGGCCTCCAGG	AAGTGCCTCTCTGCAGCTGCCGGATGGAAAC
EHMT1_e10	CCTCCAACAAGGCCCGCTCCTCGTGC	TGTGTGAAGACCACCGGGCCGCATGG
EHMT_e14	GTGTTTGTTCAGTGGACGGAATTGACCCCAA	CTTCAAATGGAGCACCAGAATAAGCGCTCTCC
EHMT1_i14	CGTTTCTTCCAGTGAAGAGTCCG	TAGTGCTGTGAATCGGGCACAGAGT
EHMT1_e16	CAGGACGCAGAGGGCTCTACGTGTT	TGCACCTGGTGCCAAGAAAGGCCA
EHMT1_e18	GAGCTTGGCTTGTGTCTGTT	CAGGAGGAGAACATTTGCCTG
EHMT1_e19	AACAAGGAAGGAGAGACGCCCCCTGCAGTGGCGAGCCT	CAACTCTCAGGTGTGGAGCGCTCTGCAGATGAGCAAGGCT
EHMT1_e20	GACAGCGAGCCATGCCCCAGCACTACAAGT	ACGTCTCTCAGAACTGCGTGACGTCCTCCAT
EHMT1_i22	GCCTGGGTTCACTACTCTCTAT	GCCTCCCTTCACTACTCTCTAT
EHMT1_e23	CTTGTCTCGAGTGAGTGAGTCCCTGGGTC	ACCCAAGCCTGGTGTCAATTTCTGGGACGGA
EHMT1_e24	GGTATGTTGGGAGCTGATTTAGACTCA	GAAGCCGACGTTCCAGAGGAAGATTCTTA
EHMT1_i25	GTTCTAAAAGTGCACCTGGGATGCGGCACGG	CAGATCGGGTGAGGAAGCTTTGGCCTTGCCTT
EHMT1_e26	CAGGTTTGACTATGGAGAGCGCT	TCTGGGACATCAAAGGCAAGCTC
CACNA1B_e1	CAACCCCATCCCGGTCAAGCAGAAGTCT	TCACCGTCAACCGCTCGCTCTTCTGCTTTC
CACNA1B_e2	GCGTCTGCCGCCAGTCTTAACTCACGCACTCCATTCAGTA	TATGATCCTGGCCACCATCATCGCCAATGCATCGTGTGGCC
CACNA1B_e6	CCAGGACCAACTTTGGCATCACCAACTTTGACAA	TATCTGTTTGCATCTTGACGGTTCGAGTGCA
CACNA1B_e11	TCTAGATTGGATCTTGTGGCGC	GGGTTCCCTAAGGTTGGA
CACNA1B_e15	GCCITCCTGTTTTCTCAGTTCAACTCCAGG	ATGAGACTCCCAACCAACTTCGACACCTTCC
CACNA1B_e20	CACACTGCCCCAGCACCTGTCTCCAGAAGTGGAGGAA	CAGCCAGAGGATGCAGACAATCAGCGGAACGCTCACTCGC
CACNA1B_e25	CAATACCATCAAGTCTCTGAGAGTCTTCTGCTCTGCGGC	CCCTCAAGACCATCAAACGGCTGCCAAGCTCAAGGTTAGA
CACNA1B_e30	GGGGTCTGGTACGTGCTTTGGTCCCTGCTTGGCTTTTGACA	ACCTATATTCTGGTTCCTCATCTGTAGGGGACCTTTGGGGCC

<sup>a</sup> The number after the “e” or “i” corresponds to the exon or the intron, respectively, in which the probe is located.

showed retained signal intensities, which indicated that the distal border of the deletion was situated between exons 6 and 11 of the *CACNA1B* gene in patient 3. The presence of the region extending from the 3' exons of *CACNA1B* toward the telomere was verified by FISH analysis, with the use of the 9qter probe from Vysis, which comprises *D9S325*, and probe RP1-112N3, which comprises *D9S2168*. Thus, patient 3 has an interstitial deletion that is flanked by *ZMYND19* (proximal) and exon 11 of the *CACNA1B* gene (distal), encompassing 380 kb. This is the smallest 9qter deletion identified so far and contains *ARRDC1*, *C9ORF37*, *EHMT1*, AK128414, and the 5' part of the *CACNA1B* gene.

Since the *EHMT1* gene was considered the most likely candidate for 9q subtelomeric deletion syndrome, we decided to sequence this gene in the remaining 20 patients in whom no deletion was identified. The GenBank reference sequence for *EHMT1* has accession number NM\_024757. The A of the ATG start codon in exon 2 is defined as “position 1” for the numbering of mutations and polymorphisms. Primers were designed to amplify all 26 exons and the three exons 15b, 27, and 28 of alternative transcripts of the gene. Primer sequences and PCR conditions are available on request. After purification with a Qiagen PCR purification kit, the PCR samples were directly sequenced on an Applied Biosystems 3730 automated sequencer, with the use of the same primers as in the PCR.

Mutation analysis identified seven sequence variants (table 2). Three of these (c.351T→C, c.951G→A, and c.996T→C) were known polymorphisms already listed in

SNP and EST databases. Another silent nucleotide transition, c.1275C→T (p.L425L), was found in 6 patients but also in 17 of 85 ethnically matched control individuals and was, therefore, considered to be a polymorphism. The c.1713G→A (p.E571E) was not reported elsewhere, but, according to several splice-site prediction programs (ESE Finder), it is unlikely to have a pathogenic effect. Unfortunately, we were not able to test the parents of the patient for this sequence change. Two nucleotide changes appeared to be causative mutations, because they disrupt the ORF of the *EHMT1* gene (fig. 2). A nonsense mutation, c.3409C→T, in exon 24 was identified in patient 4 and predicts a premature stop codon (p.R1137X). In patient 5, we identified a 13-bp deletion (1320\_1332del13) in exon 8 that causes a frameshift and a premature stop that pre-

**Table 2. Changes Found with Direct Sequencing of the *EHMT1* Gene**

DNA	Amino Acid	Exon
Pathogenic mutation:		
c.1320_1332del13	p.P442fs	8
c.3409 C→T	p.R1137X	24
Known polymorphisms:		
c.351 T→C	p.P117P	2
c.951 G→A	p.S317S	5
c.996 T→C	p.G332G	5
c.1275C→T	p.L425L	7
New polymorphism:		
c.1713G→A	p.E571E	11

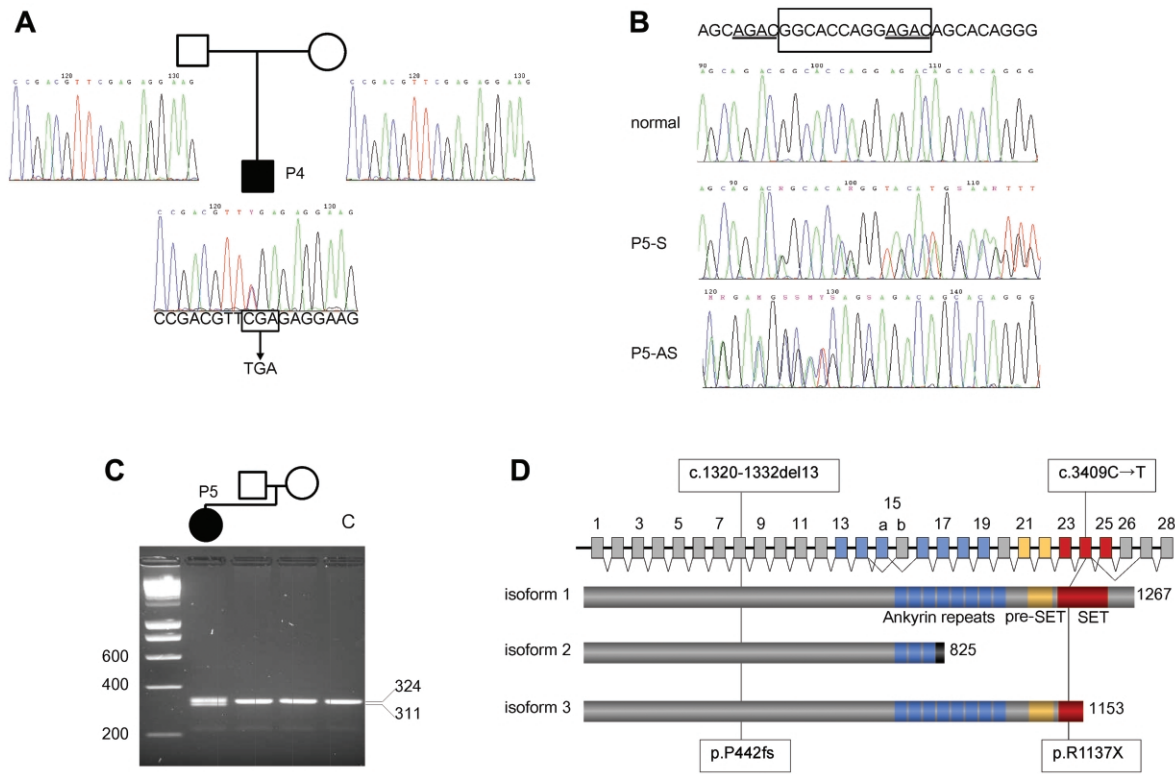


**Figure 2.** Mutations in the *EHMT1* gene identified in P4 and P5. *A*, De novo nonsense mutation identified in exon 24 of P4, which predicts premature stop codon R1137X. *B*, Deletion of 13 bp identified in exon 8 of P5. The deletion is indicated by the box. The endpoints of the deletion carry the same AGAC tetranucleotide sequence (*underlined*), which suggests that it has arisen as a result of a replication error. Top chromatogram is the sequence from a control individual; P5-S and P5-AS are the sense and antisense (reverse-complement) sequences from patient 5. *C*, Agarose gel showing that the 13-bp deletion has also occurred de novo. Sizes of the PCR products on the agarose gel: 324-bp normal exon 8 PCR product and 311-bp mutant product. Lane C is a control sample. *D*, Gene structure of the *EHMT1* gene and protein domain structure of the three predicted isoforms that result from alternative splicing. Isoform 1 is the canonical Eu-HMTase1 protein, which has eight ankyrin repeats, a pre-SET domain, and a SET domain. Isoform 2 lacks most of these recognizable C-terminal protein domains because of the use of an alternative exon 15. Isoform 3 is produced by the use of two alternative last exons. As a consequence, this isoform has an incomplete SET domain.

dicts a mutant protein of 526 aa. The two *EHMT1* gene mutations are predicted to give rise to reduced levels of functional protein because of nonsense-mediated decay of the mutant transcripts.<sup>12</sup> If such transcripts were translated, then the mutant protein would have C-terminal truncations that lack functional SET domains (fig. 2D). The p.R1137X mutation is predicted to affect the major isoform 1 and isoform 3 but not isoform 2 of the Eu-HMTase1 protein (fig. 2D).

Segregation studies performed for both mutations revealed that the changes were not present in the phenotypically normal parents. We confirmed paternity by haplotyping 15 informative markers throughout the genome, using the AmpFISTR Profiler Plus PCR Amplification Kit (Applied Biosystems) and following the manufacturer's protocol. Thus, both mutations represent de novo changes, which provides compelling evidence for their causative role.

Table 3 shows a summary of the clinical characteristics of the five patients presented in this report. Detailed clinical information is provided in appendix A (online only). In general, no major clinical differences could be observed between these 5 and the remaining 18 patients. The features of the three patients with the deletion and the two patients with the mutations that create a premature stop codon are compared with the features commonly reported in patients with a submicroscopic subtelomeric 9q deletion. All patients had typical facial dysmorphisms, including flat face with hypertelorism, eyebrow abnormalities, midfacial hypoplasia, anteverted nares, cupid bow of upper lip, and everted lower lip (fig. 3). Also, other features of the patients with the *EHMT1* mutations were reminiscent of 9q deletion syndrome, such as severe MR, seizures, and congenital heart defect. There is not an obvious disparity between the three patients with the deletion and the two patients with the intragenic mutation.

**Table 3. Clinical Features of the Five Presented Patients Compared with the Phenotypic Characteristics of 9q Subtelomeric Deletion Syndrome**

Features of 9q <sup>-</sup> Syndrome	Submicroscopic N = 30 (%)	This study				
		Deletion			<i>EHMT1</i> Mutation	
		P1	P2	P3	P4	P5
<b>General:</b>						
Age (years)	...	8	1.5	36	4	16
MR	28/28 (100)	Severe	Severe	Severe	Severe	Severe
Obesity	5 (16)	-	-	+	-	+
<b>Facial features:</b>						
Microcephaly	25 (83)	-	-	-	-	-
Brachycephaly	12 (33)	+	+	+	+	+
Flat face	5 (16)	+	+	+	+	+
Midface hypoplasia	16 (53)	+	+	+	+	+
Coarse facies	8 (27)	+	-	+	+	-
Hypertelorism	15 (50)	+	+	+	+	-
Synophrys	16 (53)	-	-	+	-	+
Downslant palpebral fissures	6 (20)	-	-	-	-	-
Upslant palpebral fissures	5 (16)	+	+	+	+	-
Arched eyebrows	8 (27)	-	-	-	-	-
Short nose	17 (57)	+	+	+	-	-
Anteverted nostrils	12 (33)	+	+	+	-	-
Carp mouth/tented lip	23 (77)	-	+	-	+	+
Macroglossia/tongue protrusion	12 (33)	-	-	+	-	-
Natal teeth	1 (3)	-	-	-	-	-
Thick/everted lower lip	5 (16)	+	+	+	+	+
Pointed chin/prognathism	5 (16)	-	-	+	+	+
Malformed ears	12 (33)	+	-	+	+	-
<b>Other features:</b>						
Brachydactyly	5 (16)	+	-	+	-	+
Simian crease	10 (30)	+	-	-	+	-
Abnormal genitals (males)	10 (33)	+	-	-	-	-
Cardiac anomaly	15 (50)	-	-	-	+	-
Anal atresia	2 (7)	-	-	-	-	-
Alopecia	3 (10)	-	-	-	-	-
Depigmentation	1 (3)	+	-	-	+	+
Renal cysts	2 (7)	-	-	-	-	-
Hydronephrosis	2 (7)	-	-	-	-	-
Behavioral problems	4 (9)	+	-	+	-	+
Sleep disturbances	3 (10)	-	-	-	-	+
Hearing loss	6 (20)	-	-	-	-	-
Hypotonia	15 (50)	+	+	+	+	+
Seizures	10 (30)	-	-	+	+	-

They each have the characteristic facial features and severe MR. On the basis of the clinical studies of these five patients, some additional features should be included in the list of characteristic features of this syndrome. The eyebrows of several patients seem straight and situated lower than usual. The designation “carp mouth” is not always justified, since the upper lip appears quite tented or shows a prominent cupid bow. Remarkably, depigmented skin patches were observed in three patients with mutations but have been reported elsewhere in only one patient.<sup>4</sup> These observations clearly underscore the fact that the prominent features of 9q deletion syndrome are caused by haploinsufficiency of a single gene rather than by a contiguous gene deletion.

It has been suggested elsewhere that specific clinical endophenotypes correlate with the extent of 9q34.3 deletion.<sup>8</sup> This correlation may be true for some rare features,

such as trigonocephaly, which has been observed in an individual with a large deletion extending proximally from the *TRAF2* gene. However, the present data clearly demonstrate that 9q<sup>-</sup> syndrome is a single-gene syndrome, not a contiguous-gene deletion syndrome. We were unable to detect any association of the extent of the deletion or of the type of mutation with specific phenotypes. For example, conotruncal heart defects and seizures are present in many patients with a 9q<sup>-</sup> telomeric deletion but were also observed in patient 4, who carries the p.R1137X nonsense mutation. The two patients with mutations are as severely affected as the three patients with deletions, and the patients with a regular 9qter deletion are as severely affected as those described in the literature. Therefore, our data do not support the use of the acronym “CHOMS” for those patients with a deletion comprising only *EHMT1* and *CACNA1B*.<sup>8</sup>





**Figure 3.** A, Patient 1 at age 8 years. B, Patient 2 at age 1 year and 6 mo. C, Patient 3 at different ages: neonate (*top left*), 11 years (*top right*), and 36 years (*bottom panels*). D, Patient 4 at different ages: 6 mo (*top left*), 18 mo (*top right*), and 4 years (*bottom panels*). E, Patient 5 at age 16 years. Note the characteristic facial dysmorphisms in all the patients. Written consent to publish these photographs was obtained from the parents of each patient.

The patients in the present study were carefully selected on the basis of the reported clinical characteristics of  $9q^-$  syndrome. This selection led to the identification of causative mutations in 5 (22%) of 23 patients, three submicroscopic deletions, and two small mutations in the *EHMT1* gene. These data emphasize the importance of careful clinical analysis before mutation analysis. Because of the hypotonia, brachycephaly, midface hypoplasia, upward slant of the eyes, and macroglossia,  $9q^-$  syndrome

may be difficult to differentiate from Down syndrome (MIM 190685), especially at birth. Furthermore, because of the facial coarseness, sleep disorders, obsessive-compulsive disorders, stereotypic movements, bursts of anger, and autohetero aggressivity,  $9q^-$  syndrome has many overlapping features with the Smith-Magenis syndrome (SMS [MIM 182290]). This overlap can be concluded also from a study on a large cohort of subtelomeric FISH studies in which, of 11 patients with a  $9q$ ter deletion, 2 patients had

a clinical diagnosis of SMS and one had a clinical diagnosis of Down syndrome.<sup>13</sup> Our data also indicate that 9q subtelomeric deletion syndrome may be a relatively common clinical entity. This finding is in line with the notion that 9q34 subtelomeric deletions comprised ~6% (11 of 175) of all subtelomeric deletions.<sup>13</sup>

Histone methylation plays an important role in modulating chromatin structure and function.<sup>14,15</sup> Histone methylation occurs on arginine and lysine residues at the N-terminal tails of histones H3 and H4. Thus far, six lysine residues located on histones H3 (lysines 4, 9, 27, 36, and 79) and H4 (lysine 20) have been reported to be sites of methylation. Lysine 9 methylation (H3-K9) is the best studied because of its fundamental role in heterochromatin formation, transcriptional silencing, X-chromosome inactivation, and DNA methylation.<sup>16</sup>

Eu-HMTase1 was identified in 2002<sup>17</sup> and was found to be closely related to the enzyme G9a. These enzymes appeared to be H3-K9 HMTases, present in euchromatic regions that formed complexes with heterochromatin protein 1 (HP1 $\alpha$  and HP1 $\gamma$ ), E2F-6, and Polycomb group (PcG) proteins.<sup>17,18</sup> It is of note that the X-linked nuclear protein, which is mutated in the  $\alpha$ -thalassemia MR syndrome (ATRX [MIM 301040]) and in several other syndromic and nonsyndromic X-linked MR (XLMR) conditions,<sup>19</sup> also interacts with HP1 and with the SET domain of the PcG protein EZH2.<sup>20</sup> Interestingly, the ATRX and related syndromes share several features with 9q<sup>-</sup> syndrome, such as severe MR, midface hypoplasia, microcephaly, cardiovascular defects, and seizures. Other genes for syndromic and nonsyndromic XLMR have been implicated in chromatin condensation as well. The methyl-CpG-binding protein 2 (MECP2) protein, which underlies Rett syndrome (MIM 312750) and nonsyndromic XLMR, is a methyl-CpG-binding protein that recruits repressor complexes and indirectly causes chromatin condensation through recruitment of histone deacetylases.<sup>21</sup> Likewise, Kruppel-associated box (KRAB) zinc-finger proteins are found in repressor complexes in euchromatic DNA, together with HP1 and another H3K9 methyltransferase, SETDB1.<sup>22</sup> Mutations in three highly related KRAB-domain zinc-finger genes are associated with XLMR.<sup>23-25</sup> It thus seems that gene silencing mediated by histone modifications are crucial for proper neuronal function and development.<sup>18</sup>

Recently, knockout mice have been generated for the *G9a* and *EHMT1* genes, which are also known as "G9a-related methyltransferase" and "*GLP*," respectively.<sup>26,27</sup> The phenotypes observed from germline mutations of the *G9a* and *EHMT1* genes were identical in many respects, including embryonic lethality, drastic reduction of H3-K9 mono- and dimethylation, induction of *MAGEA* genes, and HP1 relocalization. These and other results indicated that G9a and Eu-HMTase1 function cooperatively, probably in the same complexes, to mediate H3-K9 methylation at euchromatin. Interestingly, G9a-null embryo stem cells show altered DNA methylation in the Prader-Willi imprinted region, indicating that one or more neuronal

target genes are located in that region.<sup>28</sup> Strikingly, it was reported that no significant differences were observed between Glp<sup>+/+</sup> and Glp<sup>+/-</sup> mice and that heterozygous mice were born in Mendelian ratios. This would suggest that *EHMT1* haploinsufficiency in mice has less dramatic effects than it does in humans, although it is possible that behavioral and cognitive defects have gone unnoticed in heterozygous mice.

The findings here confirm our previous hypothesis that haploinsufficiency of the gene *EHMT1* is the cause of 9q<sup>-</sup> syndrome. Although we may have missed mutations in regulatory regions of the gene, it seems likely that mutations in other genes give rise to a similar phenotype. Likely candidate genes are those that encode components of the same histone methyltransferase complex, such as *EHMT2* encoding G9a or target genes whose expression is repressed by the chromatin remodeling activity of this complex. Functional studies are needed to give more insight into the exact pathways through which Eu-HMTase1 exerts its effects.

## Acknowledgments

This work was supported by European Union grant QL3-CT-2002-01810 (EURO-MRX) (to H.v.B.), the Hersenstichting Nederland grant 12F04(2) (to H.v.B.), and ZonMw grant 907-00-058 (to B.B.A.d.V.). We thank W. Reardon, L. Brueton, T. Cole, F. Faravelli, G. Gillessen-Kaesbach, A. Delicado, G. Houge, T. Prescott, and M. Badura, for referrals of patients.

## Web Resources

The accession number and URLs for data presented herein are as follows:

ESE Finder, <http://www.genet.sickkids.on.ca/>

GenBank, <http://www.ncbi.nlm.nih.gov/Genbank/> (for *EHMT1* [accession number NM\_024757])

MRC-Holland, <http://www.mrc-holland.com/>

NCBI Unified Library Database (UNILIB), <http://www.ncbi.nlm.nih.gov/>

Online Mendelian Inheritance in Man (OMIM), <http://www.ncbi.nlm.nih.gov/Omim/> (for Eu-HMTase1, Down syndrome, SMS, ATRX, and Rett syndrome)

UCSC Genome Browser (Golden Path), <http://genome.cse.ucsc.edu/> (May 2004 Build)

## References

1. Harada N, Hatchwell E, Okamoto N, Tsukahara M, Kurosawa K, Kawame H, Kondoh T, Ohashi H, Tsukino R, Kondoh Y, Shimokawa O, Ida T, Nagai T, Fukushima Y, Yoshiura K, Niikawa N, Matsumoto N (2004) Subtelomere specific microarray based comparative genomic hybridisation: a rapid detection system for cryptic rearrangements in idiopathic mental retardation. *J Med Genet* 41:130-136
2. Harada N, Visser R, Dawson A, Fukamachi M, Iwakoshi M, Okamoto N, Kishino T, Niikawa N, Matsumoto N (2004) A 1-Mb critical region in six patients with 9q34.3 terminal deletion syndrome. *J Hum Genet* 49:440-444
3. Iwakoshi M, Okamoto N, Harada N, Nakamura T, Yamamori

- S, Fujita H, Niikawa N, Matsumoto N (2004) 9q34.3 Deletion syndrome in three unrelated children. *Am J Med Genet A* 126:278–283
4. Stewart DR, Huang A, Faravelli F, Anderlid BM, Medne L, Ciprero K, Kaur M, Rossi E, Tenconi R, Nordenskjold M, Gripp KW, Nicholson L, Meschino WS, Capua E, Quarrell OW, Flint J, Irons M, Giampietro PF, Schowalter DB, Zaleski CA, Malacarne M, Zackai EH, Spinner NB, Krantz ID (2004) Subtelomeric deletions of chromosome 9q: a novel microdeletion syndrome. *Am J Med Genet A* 128:340–351
  5. Neas KR, Smith JM, Chia N, Huseyin S, St. Heaps L, Peters G, Sholler G, Tzioumi D, Sillence DO, Mowat D (2005) Three patients with terminal deletions within the subtelomeric region of chromosome 9q. *Am J Med Genet A* 132:425–430
  6. Kleefstra T, Smidt M, Banning MJ, Oudakker AR, Van Esch H, de Brouwer AP, Nillesen W, Sistermans EA, Hamel BC, de Bruijn D, Fryns JP, Yntema HG, Brunner HG, de Vries BB, van Bokhoven H (2005) Disruption of the gene euchromatin histone methyl transferase1 (Eu-HMTase1) is associated with the 9q34 subtelomeric deletion syndrome. *J Med Genet* 42:299–306
  7. Kleefstra T, Koolen DA, Nillesen WM, de Leeuw N, Hamel BC, Veltman JA, Sistermans EA, van Bokhoven H, van Ravenswaay C, de Vries BB (2006) Interstitial 2.2 Mb deletion at 9q34 in a patient with mental retardation but without classical features of the 9q subtelomeric deletion syndrome. *Am J Med Genet A* 140:618–623
  8. Yatsenko SA, Cheung SW, Scott DA, Nowaczyk MJ, Tarnopolsky M, Naidu S, Bibat G, Patel A, Leroy JG, Scaglia F, Stanekiewicz P, Lupski JR (2005) Deletion 9q34.3 syndrome: genotype-phenotype correlations and an extended deletion in a patient with features of Opitz C trigonocephaly. *J Med Genet* 42:328–335
  9. Koolen DA, Nillesen WM, Versteeg MH, Merckx GF, Knoers NV, Kets M, Vermeer S, van Ravenswaaij CM, de Kovel CG, Brunner HG, Smeets D, de Vries BB, Sistermans EA (2004) Screening for subtelomeric rearrangements in 210 patients with unexplained mental retardation using multiplex ligation dependent probe amplification (MLPA). *J Med Genet* 41: 892–899
  10. Miller SA, Dykes DD, Polesky HF (1988) A simple salting out procedure for extracting DNA from human nucleated cells. *Nucleic Acids Res* 16:1215
  11. Schouten JP, McElgunn CJ, Waaijer R, Zwijnenburg D, Diepvens F, Pals G (2002) Relative quantification of 40 nucleic acid sequences by multiplex ligation-dependent probe amplification. *Nucleic Acids Res* 30:e57
  12. Baker KE, Parker R (2004) Nonsense-mediated mRNA decay: terminating erroneous gene expression. *Curr Opin Cell Biol* 16:293–299
  13. Ravnán JB, Tepperberg JH, Papenhausen P, Lamb AN, Hedrick J, Eash D, Ledbetter DH, Martin CL (2005) Subtelomere FISH analysis of 11,688 cases: an evaluation of the frequency and pattern of subtelomere rearrangements in individuals with developmental disabilities. *J Med Genet* (<http://jmg.bmjournals.com/cgi/rapidpdf/jmg.2005.036350v1>) (electronically published September 30, 2005) (accessed May 25, 2006)
  14. Lachner M, Jenuwein T (2002) The many faces of histone lysine methylation. *Curr Opin Cell Biol* 14:286–298
  15. Lachner M, O'Sullivan RJ, Jenuwein T (2003) An epigenetic road map for histone lysine methylation. *J Cell Sci* 116:2117–2124
  16. Richards EJ, Elgin SC (2002) Epigenetic codes for heterochromatin formation and silencing: rounding up the usual suspects. *Cell* 108:489–500
  17. Ogawa H, Ishiguro K, Gaubatz S, Livingston DM, Nakatani Y (2002) A complex with chromatin modifiers that occupies E2F- and Myc-responsive genes in G0 cells. *Science* 296:1132–1136
  18. Roopra A, Qazi R, Schoenike B, Daley TJ, Morisson JF (2004) localized domains of G9a-mediated histone methylation are required for silencing neuronal genes. *Mol Cell* 14:727–738
  19. Gibbons RJ, Higgs DR (2000) Molecular-clinical spectrum of the ATR-X syndrome. *Am J Med Genet* 97:204–212
  20. Cardoso C, Timsit S, Villard L, Khrestchatisky M, Fontes M, Colleaux L (1998) Specific interaction between the XNP/ATR-X gene product and the SET domain of the human EZH2 protein. *Hum Mol Genet* 7:679–684
  21. Shahbazian MD, Zoghbi HY (2002) Rett syndrome and MeCP2: linking epigenetics and neuronal function. *Am J Hum Genet* 71:1259–1272
  22. Schultz DC, Ayyanathan K, Negorev D, Maul GG, Rauscher FJ 3rd (2002) SETDB1: a novel KAP-1-associated histone H3, lysine 9-specific methyltransferase that contributes to HP1-mediated silencing of euchromatic genes by KRAB zinc-finger proteins. *Genes Dev* 16:919–932
  23. Shoichet SA, Hoffmann K, Menzel C, Trautmann U, Moser B, Hoeltzenbein M, Echenne B, Partington M, Van Bokhoven H, Moraine C, Fryns JP, Chelly J, Rott HD, Ropers HH, Kalscheuer VM (2003) Mutations in the *ZNF41* gene are associated with cognitive deficits: identification of a new candidate for X-linked mental retardation. *Am J Hum Genet* 73: 1341–1354
  24. Kleefstra T, Yntema HG, Oudakker AR, Banning MJ, Kalscheuer VM, Chelly J, Moraine C, Ropers HH, Fryns JP, Jansen IM, Sistermans EA, Nillesen WN, de Vries LB, Hamel BC, van Bokhoven H (2004) Zinc finger 81 (*ZNF81*) mutations associated with X-linked mental retardation. *J Med Genet* 41: 394–399
  25. Lugtenberg D, Yntema HG, Banning MJ, Oudakker AR, Firth HV, Willatt L, Raynaud M, Kleefstra T, Fryns JP, Ropers HH, Chelly J, Moraine C, Gecz J, Reeuwijk J, Nabuurs SB, de Vries BB, Hamel BC, de Brouwer AP, Bokhoven H (2006) *ZNF674*: a new Kruppel-associated box-containing zinc-finger gene involved in nonsyndromic X-linked mental retardation. *Am J Hum Genet* 78:265–278
  26. Tachibana M, Ueda J, Fukuda M, Takeda N, Ohta T, Iwanari H, Sakihama T, Kodama T, Hamakubo T, Shinkai Y (2005) Histone methyltransferases G9a and GLP form heteromeric complexes and are both crucial for methylation of euchromatin at H3-K9. *Genes Dev* 19:815–826
  27. Tachibana M, Sugimoto K, Nozaki M, Ueda J, Ohta T, Ohki M, Fukuda M, Takeda N, Niida H, Kato H, Shinkai Y (2002) Histone methyltransferase plays a dominant role in euchromatic histone H3 lysine 9 methylation and is essential for early embryogenesis. *Genes Dev* 16:1779–1791
  28. Xin Z, Tachibana M, Guggiari M, Heard E, Shinkai Y, Wagstaff J (2003) Role of histone methyltransferase G9a in CpG methylation of the Prader-Willi syndrome imprinting center. *J Biol Chem* 278:14996–15000